 DOI: 10.1002/masy.200651029

Ultrasonic Investigation of the Gelation Process of Poly(Acrylamide) Gels

Tomohisa Norisuye,[*1] *Anatoliy Strybulevych,*[2] *Martin Scanlon,*[3] *John Page*[2]

Summary: The time evolution of ultrasonic velocity and attenuation has been investigated in-situ during the gelation process of polyacrylamide (PAAm) hydrogels. Longitudinal ultrasonic pulses were transmitted through the gel samples and continuously recorded to obtain the magnitude and phase of the waves as a function of time and frequency, enabling the attenuation coefficient, α, and phase velocity, v_p, of PAAm gels to be determined. The reaction was characterized by (1) an initial rapid increase in α and v_p, and (2) a subsequent reduction after both quantities passed through a peak associated with the exothermic reaction for the PAAm gelation. The square of v_p is proportional to the longitudinal modulus of the sample and inversely proportional to the density, and the values of v_p for the aged gels were smaller than those before the gelation. The cross-linker concentration dependence was further examined in order to investigate the gelation process accompanied by phase separation.

Keywords: acrylamide; gelation; ultrasonic

Introduction

Polymer gels are generally produced by (I) copolymerization of a monomer and a cross-linker in the presence of a solvent or (II) introduction of cross-links into a homogenous polymer solution.[1] In either case, gelation leads to a well-developed three-dimensional network swollen in a solvent. Polyacrylamide (PAAm) gel is one of the most popular gels in the field of protein separation or medical applications. As a result, the rheological and structural properties of the PAAm gels have been well investigated by many scientists from chemical and physical points of view.[2–5] In general, PAAms are synthesized with acrylamide (AAm) and bisacrylamide (BIS) as starting compounds, so that PAAms can be classified as group I gels. Unlike the ideal network structure, which is often taken to be a mesh-like structure, this type of gel is microscopically heterogeneous because of the presence of micro-gel clusters consisting of intra-molecularly cross-linked elements. This structure has been explained in terms of free-radical polymerization and/or a difference of the reactivity ratio of the compounds in the copolymerization.[6–8] On the contrary, less heterogeneous gels can be made if the cross-links are introduced in a homogeneous solution (case II). Note that the gels are inherently heterogeneous irrespective of the reaction method because of the fact that the concentration fluctuations are frozen at onset of gelation, resulting in the scattering of light, x-rays and neutrons.[1] Interestingly, the monomer cross-linking method seems to be suitable for sieving or separation applications in spite of the strong heterogeneities.

Monitoring of the gelation process is one of the most important strategies to understand how and when the gel structure is

[1] Department of Macromolecular Science and Engineering, Kyoto Institute of Technology, Sakyo-ku, Kyoto, Japan
Tel & Fax: (+81) 75 724 7853
E-mail: nori@kit.jp
[2] Department of Physics and Astronomy, University of Manitoba, Winnipeg, MB, Canada
[3] Department of Food Science, University of Manitoba, Winnipeg, MB, Canada

formed.[2,9] While light scattering techniques and rheology have been developed and applied during the last decade, these methods are limited to systems that are transparent or stable against shear, respectively. For example, static light scattering cannot be used on opaque samples because of the strong attenuation of the light source and the complexity of multiple scattering. On the other hand, rheological measurements apply mechanical shear to the samples, resulting in ambiguity of the determination of the gel point and the critical behavior for weak materials during the reaction. More recently a low-shear oscillatory technique was proposed to overcome the problem.[10] However, there is still a strong need for methods that can detect gelation without contacting the sample, so that the physical properties of weak materials, such as fragile aggregates, physical gels or foam, can be investigated. Therefore ultrasonic spectroscopy is a promising tool to monitor the gelation process without disturbing the system. It also can be a complementary tool for traditional rheology and light scattering. So far, ultrasonic spectroscopy has been applied to investigate gelation in a number of systems, including protein, natural hydrocolloids, polyurethane, epoxy, gelatin and AAm.[11–15] However, most of those reactions were induced by temperature variation, so that the results involved the temperature dependence of ultrasound properties in addition to those directly attributed to gelation. PAAm can be considered as a model monomer cross-linking system, which is expected to be well-suited for studying percolation phenomena since the experiment is performed in a constant temperature environment. In this paper, we will demonstrate the applicability of ultrasound to monitor the reaction process of the PAAm system in-situ for a wide range of the cross-linker concentrations, including those for which phase separation occurs.

Experimental

Synthesis of AAm Gels

Acrylamide (AAm), *N*-*N*′-methylenbismethylenbisacrylamide (BIS), ammonium persulfate (APS) and tetramethylethylenediamine (TEMED) were purchased from Aldrich and were used as received. Prescribed amount of AAm, BIS and APS were dissolved in distilled water, where the AAm concentration, C_{AAm}, was fixed to be 0.8 g/10ml and the BIS concentration, C_{BIS}, was varied in range $0 \sim 0.14$ g/10ml. The stock solution was degassed to eliminate oxygen, which would prevent the reaction from occurring. Although the solution should usually be stored in refrigerator in order to stabilize the sample before the addition of TEMED, this procedure inevitably leads to an initial temperature rise of the sample when placed in the reaction bath, potentially making it difficult to separate the contributions to the measured signal due to temperature changes from those due to gelation. Therefore the solution was aged in the reaction bath in order to match the temperature of the stock solution with the reaction bath. After the addition of TEMED, the mixture was poured into a rectangular plastic cell with a sample thickness of 10 mm and the wall thickness of 1mm, followed by immersion of the sealed sample into a thermostat bath. Then the reaction was monitored at $27.7 \pm 0.01\,^{\circ}C$ using the ultrasonic setup described in the next section. The sample became opaque when C_{BIS} exceeded 0.08 g/10ml.

Ultrasonic Spectroscopy

An arbitrary wave generator (33220A: Agilent) and a broadband amplifier (Model 250L: Amplifier Research) were employed to generate and amplify the signal applied to the generating ultrasound transducer. A cosine wave convolved with a Gaussian function was employed as an input pulse. A trigger pulse from the arbitrary waveform generator was connected to a digital oscilloscope (Tektronix TDS544A), while the ultrasonic pulse was transmitted through the sample, which was placed between generating and receiving transducers. This allowed synchronous recording of the ultrasound signals with respect to the trigger pulse. Two plane wave transducers (20 MHz, longitudinal waves) were used to generate and detect the ultrasound waves.

Results and Discussion

Figure 1(a) shows examples of longitudinal ultrasound pulses received by the 20 MHz plane wave transducer. The reference signal was obtained with pure water in the plastic sample cell. Pulses were detected at approximately 4.4 μs and 5.2 μs respectively in Fig. 1(a), corresponding to the main waveform and the reflected signal within a single wall. Traditionally, the transmitted signals can be analyzed directly in the time domain by using the amplitude and arrival time of the phase oscillations. However, in our case, since the attenuation and the time shift of the signal were so small, we employed a fast Fourier transform (FFT) method to extract the amplitude and phase with high accuracy over the entire frequency bandwidth of the pulses. Spurious pulses, such as the signal from wall reflections and noise outside the range of times containing the main pulse, were truncated before taking the FFTs. Figure 1(b) shows the FFT magnitude of the sample and reference. The peak appeared at around 19 MHz with a −6dB range of 18 ~ 20MHz. No noticeable frequency shift or shape change was detected in the magnitude throughout the gelation process.

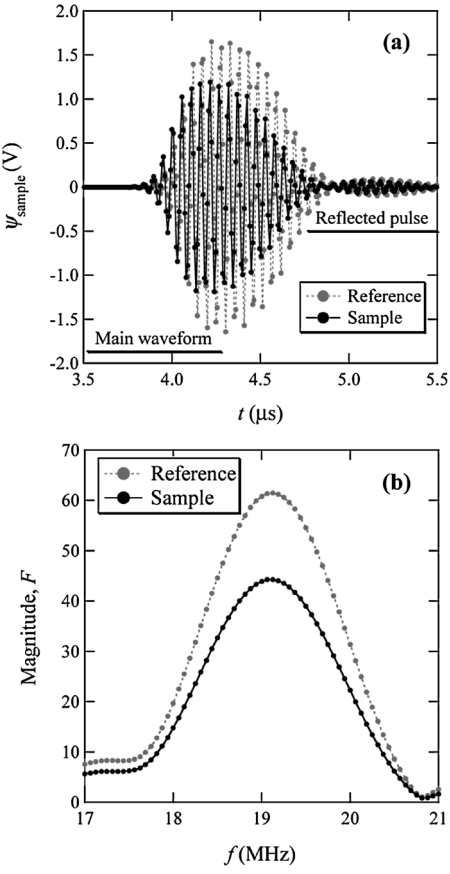

Figure 1.
(a) Examples of longitudinal ultrasound pulses received by a 20 MHz plane wave transducer. (b) The FFT magnitude of the sample and reference.

Figures 2 (a) and (b) respectively show the attenuation coefficient, α, and the phase velocity, v_p, given by,

$$\alpha = -2\ln(F_S/F_R)/L \quad (1)$$

$$v_p = 2\pi Lf/(\phi_S - \phi_R + 2n\pi) \quad (2)$$

as a function of the frequency, where F, ϕ, and L are the Fourier magnitude, cumulative phase and the sample thickness, respectively, and the subscript S and R represent the sample and reference. Note that eq. (2) contains an unknown multiple of 2π, which stems from the difficulty in unambiguously determining the cumulative phase in samples that are many wavelengths thick. In order to determine the proper value of n, the group velocity was calculated according to the following steps[16]. First, the Fourier spectrum of the original pulse was multiplied by a Gaussian function with a certain width and central frequency in order to filter the pulse. After taking the inverse Fourier transformation, the time difference between the filtered pulses for the sample and reference was measured to obtain the group velocity, v_g. The frequency dependence of v_g is plotted with the open symbols in Figure 2(b). As can be seen from the figure, v_g is very close to the middle estimate of v_p. Although the phase and group velocities are not always the same, they are quite similar to each other unless there is significant dispersion.[16,17] Thus, this comparison of v_p and v_g allows v_p to be correctly determined as the middle estimate, shown by the solid symbols in Fig. 2(b); this result corresponds to the value of n that gives a flat

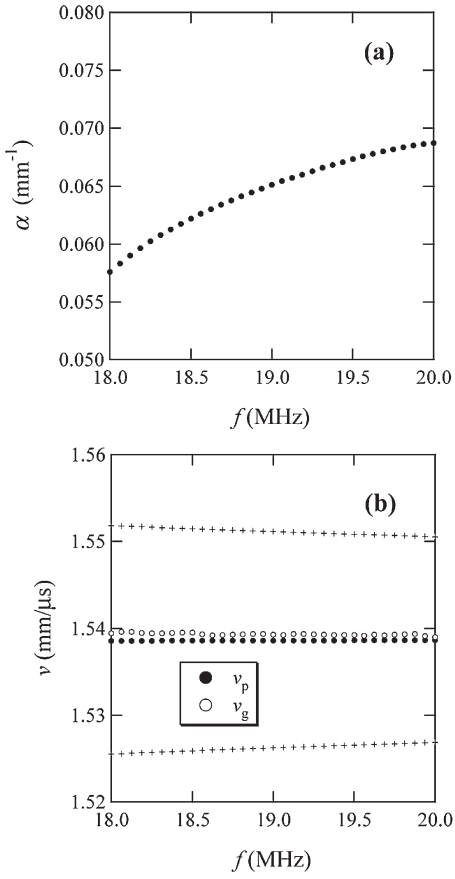

Figure 2.
(a) The attenuation coefficient, α, and (b) the phase velocity, v_p, as a function of the frequency. These data were taken on a sample with the highest cross-linker concentration, at a long time after gelation. In (b), v_p is represented by the solid circles and v_g by the open circles, with the crosses representing estimates of v_p that include either one too many or one too few multiples of 2π the cumulative phase (see Eq. (2)).

frequency dependence for v_p (i.e. v_p independent of frequency), which is the natural choice for n in a non-dispersive medium.

Figure 3 (a) and (b) demonstrate the time course of α and v_p with different cross-linker concentrations. The reaction was characterized by a sharp rise in α and v_p, followed by a gradual reduction. Note that the slower increases in v_p seen in the early stage of the reaction was due to an inevitable temperature mismatch between the sample and the thermostat bath. Although the samples were aged at the same temperature, there was a small temperature drop during addition of the catalyst, and hence a small temperature rise once the sample cell was re-immersed in the reaction bath. The emergence of the peak in α may be explained as an initial increase in the viscosity and subsequent increase in the elasticity during gelation. An experiment for $c_{BIS} = 0.14$ (g/10 mL) without any catalyst was also performed as a control. Surprisingly, the plateau value of v_p for the gel was lower than that of the monomer solution without the catalyst. Since $v_p = \sqrt{\beta'/\rho}$, where β' is the real part of the longitudinal modulus and ρ is the density, this suggests that either the density increases or the longitudinal modulus becomes smaller during the reaction. It is likely that the dominant effect is the increase in the

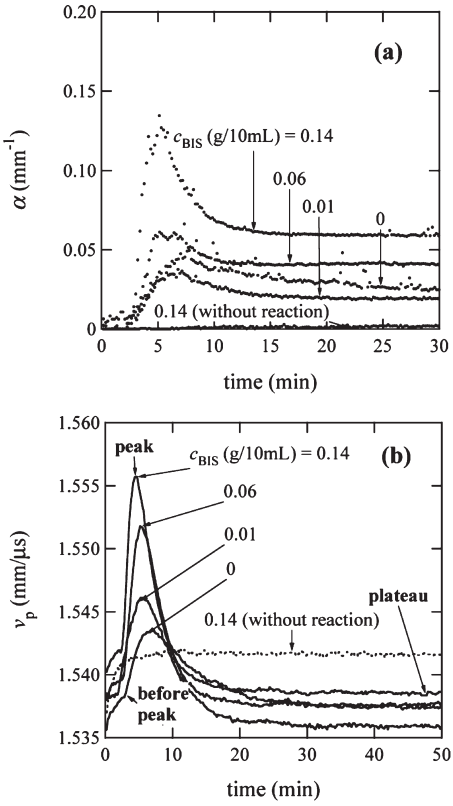

Figure 3.
The time course of α and v_p with different cross-linker concentrations.

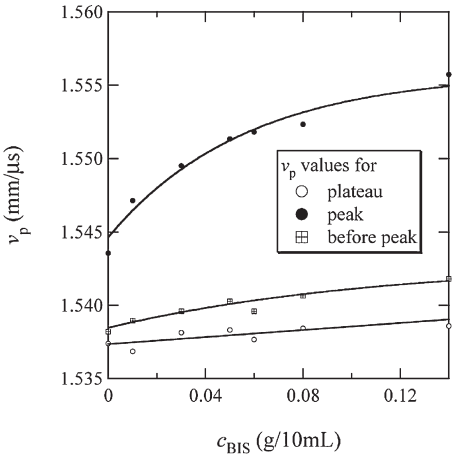

Figure 4.
The c_{BIS} dependence of v_p, sampled before the peak, at the peak and in the plateau.

density, since the inter-monomer distance generally becomes shorter by the formation of covalent bonds during polymerization, and it is difficult to envisage how the gel would become more compressive than the monomer solution in this concentration range. Note that PAAm gels are elastically weak, so that the contribution of the shear modulus of the gel to its longitudinal modulus is too small to measure and does not affect the velocity changes seen in Fig. 3.

Figure 4 summarizes the c_{BIS} dependence of v_p, sampled at three times during the gelation process. The peak value of v_p systematically increased with c_{BIS}, with the rate of increase leveling off at the higher c_{BIS}. In addition, v_p of the initial and plateau values also exhibited a rise, although the c_{BIS} dependence was quite weak compared with that of the peak. It should be noted that the plateau value was always smaller than the initial value irrespective of the cross-linker concentration. Here one can speculate on the following possibilities to explain the emergence of the peak of v_p: (i) a velocity increase due to the chain overlap and entanglement, (ii) formation of higher elastic or density domains and (iii) a temperature change due to the exothermic

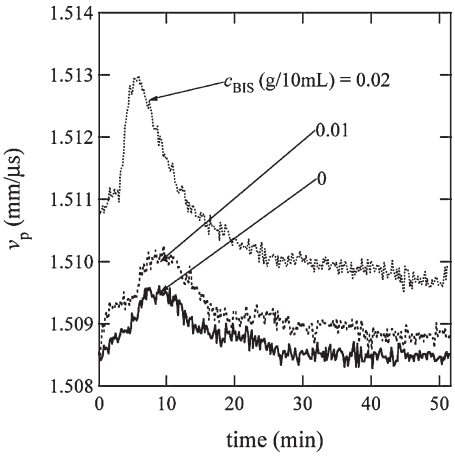

Figure 5.
The time course of v_p with different cross-linker concentrations and a sufficiently low total concentration to prevent entanglement of the polymer chains.

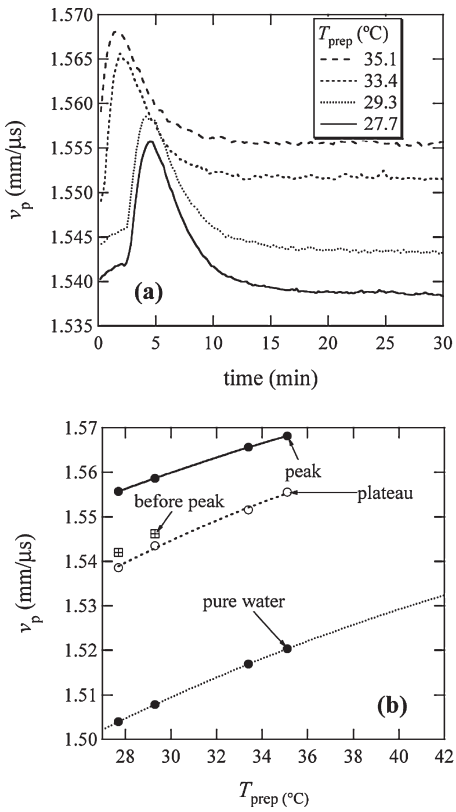

Figure 6.
The time-course of v_p with different preparation temperatures, T_{prep}.

reaction. In order to consider the possibility of case (i) ocurring, the gel concentration dependence was examined.

Figure 5 shows that PAAm gels with different cross-linker concentrations have a similar reaction time dependence, even though the total concentration was reduced to 0.1 g/10ml, which was far below the concentration for entanglement of the polymer chains. As shown in the figure, a peak in v_p was also found in the time course for this concentration, suggesting that topological constraints or physical interactions in the polymer chains were not the main cause of the appearance of the peak in v_p. The peak was more pronounced with increasing the cross-linker concentration. Note that these samples remained in the sol state even after a long aging time.

Subsequently, the preparation temperature dependence was examined. Figure 6(a) shows the time-course of v_p with different preparation temperatures, T_{prep}. Since the reaction proceeded very quickly for the higher temperatures, the initial variation of v_p was not detected for $T_{prep} = 33.4$ and 35.1 °C. In Figure 6(b), v_p for the peak and plateau is exhibited together with the data for pure water taken from a reference[18]. The temperature dependence of the sound velocity for water was fitted by a polynomial function. A similar T_{prep} dependence was also found for the polyAAm gels, although the values of v_p were higher than those of pure water due to the concentration effect of AAm and BIS. By taking account of the fact that we did observe this kind of peak even in the low gel concentration regime, the origin of the peak was attributed to temperature changes due to an exothermic reaction for the monomer cross-linking system, rather than the characteristics of gelation.

In order to investigate the reaction process over a broader range of ultrasonic frequencies, a 2.25 MHz-transducer and a hydrophone were employed as source generator and detector, respectively. Figure 7 shows the c_{BIS} dependencies of v_p at the peak, before the peak and in the plateau. Here two series of samples were examined: (1) the same set of concentrations used in the 20MHz experiments and (2) doubled concentrations for all the reagents. While,

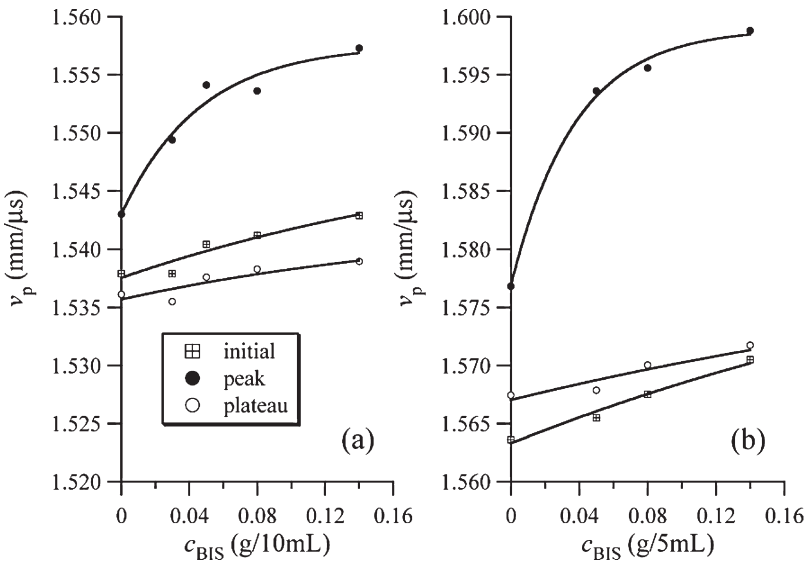

Figure 7.

c_{BIS} dependence of v_p at the peak, before the peak and in the plateau for (a) the standard concentration and for (b) a doubled concentration.

in the first case, v_p is quite similar to the 20 MHz data, the latter exhibited larger values due to the higher monomer concentration (right). Interestingly, inflection of v_p before the peak and at the plateau was not observed when the concentration was doubled. In this case, the plateau value was higher than the initial value for the weaker gels. The difference becomes smaller with increasing c_{BIS}.

In contrast to the behaviour of the velocity, the peak in the attenuation cannot be directly ascribed to the sample temperature rise during gelation, as the experiments in which the preparation temperature was varied did not show a corresponding increase in attenuation. For low attenuation systems, the real and imaginary parts of the longitudinal moduli, β' and β'', are related to the velocity and attenuation by:

$$\beta' = \rho v^2 = K' + \frac{4}{3}G' \tag{3}$$

$$\frac{\beta''}{\omega} = \frac{2\rho\alpha v^3}{\omega^2} = \zeta + \frac{4}{3}\eta \tag{4}$$

where K' and G' are the real parts of the bulk and shear moduli, respectively, ω is the angular frequency, and ζ and η are the bulk viscosity and shear viscosity, respectively. Thus the attenuation is related directly to the viscosity, so that the attenuation peak is likely related to the large changes in the viscosity near the gel point. However, we do not see evidence of critical behaviour of the viscosity near the gel point, as has been seen in some other systems[13,19,20]. The time evolution of the moduli may be inferred from Fig. 8, where $\alpha v^3/f^2$ and v^2 are plotted as a function of time for several frequencies between 18.5 and 20 MHz. Before the peak, the data are consistent with a frequency squared dependence of the attenuation, while at longer times the data in Fig. 8(a) do not superpose, indicating a weaker frequency dependence. This long time behaviour of the attenuation can be ascribed to an additional mechanism, which is important, especially at high frequencies, once the gel is formed[15]. This contribution to the plateau attenuation arises from frictional losses due to the relative motion of the liquid matrix and the PAAm network as the ultrasonic wave passes through the gel.

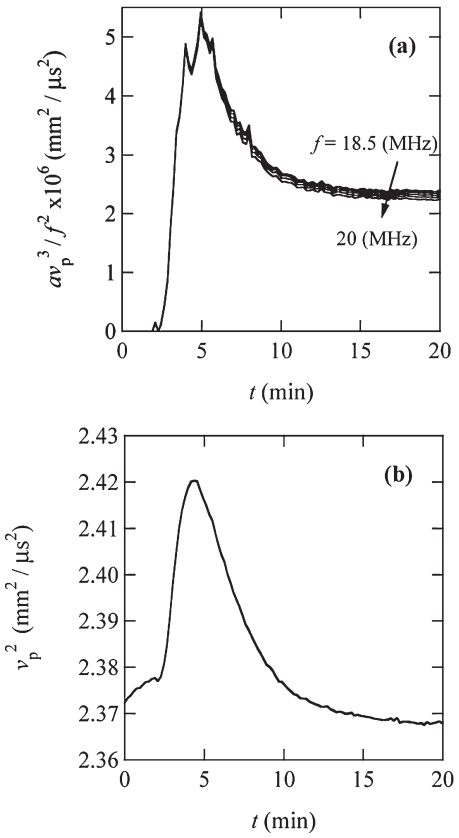

Figure 8.
The time evolution of $\alpha v^3/f^2$ and v^2, which are proportional to the longitudinal moduli.

Conclusions

In-situ monitoring of the gelation process of acrylamide gels has been carried out by means of ultrasonic spectroscopy using 20 MHz longitudinal waves. Although the changes in velocity and attenuation were very small, the time evolution of these ultrasonic parameters was successfully extracted throughout the reaction with the aid of a broadband technique. Pronounced peaks in the ultrasonic attenuation coefficient and phase velocity were found during the time course. While the peak in

the attenuation coefficient can be explained by the viscosity increase and subsequent enhancement of the elasticity during the reaction, the peak in the phase velocity was unusual. Although we studied the gelation without changing the temperature of the thermostat bath, this behavior was attributed to the exothermic reaction of the PAAm. In other words, ultrasonic spectroscopy with a longitudinal setup is suitable for observing an exothermic or endothermic reaction process. This will help to understand the timing of reactions for new class of materials containing more than two reacting components. If we can further apply this method by moving the sampling position across the surface of the gel, it will offer a possibility to build a 3D temperature diffusion profile to understand how and when the heat diffuses out.

Acknowledgements: Support from NSERC is gratefully acknowledged. This work is supported by Grant-in-Aid, No. 16750189 (to TN) from the Ministry of Education, Science, Sports, Culture, and Technology.

[1] Norisuye, T.; Kida, Y.; Masui, N.; Tran-Cong-Miyata, Q.; *Macromolecules* **2003**, *36*, 6202.
[2] Calvet, D.; Wong, J. Y.; Giasson, S.; *Macromolecules* **2004**, *37*, 7762.
[3] Dasgupta, B. R.; Weitz, D. A.; *Physical Review E* **2005**, *71*, 021504.
[4] Mallam, S.; Horkay, F.; Hecht, A. M.; Geissler, E.; *Macromolecules* **1989**, *22*, 3356.
[5] Kizilay, M. Y.; Okay, O.; *Macromolecules* **2003**, *36*, 6856.
[6] Ide, N.; Fukuda, T.; *Macromolecules* **1999**, *32*, 95.
[7] Naghash, H. J.; Okay, O.; *J. Appl. Polym. Sci.* **1996**, *60*, 971.
[8] Patras, G.; Qiao, G. G.; Solomon, D. H.; *Macromolecules* **2001**, *34*, 6369.
[9] Shibayama, M.; Norisuye, T.; *Bull. Chem. Soc. Jpn.* **2002**, *75*, 641.
[10] Richter, S.; Matzker, R.; Schroter, K.; *Macromolecular Rapid Communications* **2005**, *26*, 1626.
[11] Baillif, P. Y.; Tabellout, M.; Emery, J. R.; *Macromolecules* **1999**, *32*, 3432.
[12] Corredig, M.; Alexander, M.; Dalgleish, D. G.; *Food Research International* **2004**, *37*, 557.
[13] Sidebottom, D. L.; *Physical Review E* **1993**, *48*, 391.
[14] Toubal, M.; Nongaillard, B.; Radziszewski, E.; Boulenguer, P.; Langendorff, V.; *Journal of Food Engineering* **2003**, *58*, 1.
[15] Bacri, J.-C.; Courdille, J.-M.; Dumas, J.; Rajaonarison, R.; *J. Physique* **1980**, *41*, L369
[16] Page, J. H.; Sheng, P.; Schriemer, H. P.; Jones, I.; Jing, X.; Weitz, D. A.; *Science* **1996**, *271*, 634
[17] Povey, M. J. W.; Ultrasonic Techniques for Fluids Characterization: Academic Press; **1997**.
[18] Slutsky, L. J.; Ultrasonic chemical relaxation spectroscopy Methods of Experimental Physics: New York: Academic; **1981**; Vol. *19*.
[19] Winter, H. H.; Mours, M.; *Adv. Polym. Sci.* **1997**, *134*, 167.
[20] Antonietti, M.; Foelsch, K. J.; Sillescu, H.; Pakula, T.; *Macromolecules* **1989**, *22*, 2812.

